EUROPEAN JOURNAL OF CANCER 44 (2008) 740–749

available at www.sciencedirect.com

journal homepage: www.ejconline.com

Effects of FR235222, a novel HDAC inhibitor, in proliferation and apoptosis of human leukaemia cell lines: Role of Annexin A1

Antonello Petrella[a,*,c], *Cosimo Walter D'Acunto*[a,c], *Manuela Rodriquez*[a], *Michela Festa*[a], *Alessandra Tosco*[a], *Ines Bruno*[a], *Stefania Terracciano*[a], *Maurizio Taddei*[b], *Luigi Gomez Paloma*[a], *Luca Parente*[a]

[a]*Dipartimento di Scienze Farmaceutiche, Università di Salerno, Via Ponte Don Melillo, 84084 Fisciano, Salerno, Italy*
[b]*Dipartimento Farmaco Chimico Tecnologico, Università di Siena, Siena, Italy*

ARTICLE INFO

Article history:
Received 12 December 2007
Received in revised form
24 January 2008
Accepted 28 January 2008
Available online 4 March 2008

Keywords:
Annexin A1
Histone deacetylase inhibitors
Leukaemia cell lines
Cell proliferation
Apoptosis

ABSTRACT

FR235222, a novel histone deacetylase inhibitor (HDACi), at 50 nM caused accumulation of acetylated histone H4, inhibition of cell proliferation and G1 cycle arrest accompanied by increase of p21 and down-regulation of cyclin E in human promyelocytic leukaemia U937 cells. The compound was also able to increase the protein and mRNA levels of annexin A1 (ANXA1) without effects on apoptosis. Similar effects were observed in human chronic myelogenous leukaemia K562 cells and human T cell leukaemia Jurkat cells. Cycle arrest and ANXA1 expression, without significant effects on apoptosis, were also induced by different HDACi like suberoylanilide hydroxamic acid (SAHA) and trichostatin-A (TSA). FR235222 at 0.5 μM stimulated apoptosis of all leukaemia cell lines associated to an increased expression of the full-length (37 kDa) protein and the appearance of a 33 kDa N-terminal cleavage product in both cytosol and membrane. These results suggest that ANXA1 expression may mediate cycle arrest induced by low doses FR235222, whereas apoptosis induced by high doses FR235222 is associated to ANXA1 processing.

1. Introduction

Annexin A1 (ANXA1, lipocortin-1) is the first characterised member of the annexin superfamily of proteins, so called since their main property is to bind (i.e. to annex) to cellular membranes in a Ca^{2+}-dependent manner. Originally described as a phospholipase A2-inhibitory protein, ANXA1 can affect many components of the inflammatory reaction besides the metabolism of arachidonic acid. Moreover, it has been involved in a broad range of molecular and cellular processes,[1] including kinase activities in signal transductions, the maintenance of cytoskeleton and extracellular matrix integrity, tissue growth and differentiation. A role for ANXA1 in apoptosis and cancer has also been recently proposed (for reviews see Refs. 2,3). The over-expression of ANXA1 in U937 cells and in broncho-alveolar epithelial cells promoted apoptosis associated with caspase-3 activation.[4,5] ANXA1 is commonly deregulated in several cancers; indeed, ANXA1 is

* *Corresponding author:* Tel.: +39 089 969762; fax: +39 089 969602.
E-mail address: apetrella@unisa.it (A. Petrella).
[c] These authors contributed equally to the paper.
0959-8049/$ - see front matter
doi:10.1016/j.ejca.2008.01.023

markedly down-regulated in oesophageal, prostate and gastric carcinomas.[6–8] The relation between ANXA1 down-regulation and tumour differentiation has been observed by us in thyroid cancer[9] and by others in head and neck cancer.[10] Although the role of ANXA1 in cancer development has not been well characterised, the diminished ANXA1 expression in several types of cancers suggests that ANXA1 may be a negative regulator of cancer cell growth.[8,11] The cause of reduced ANXA1 protein expression is still not well understood. Possible mechanisms include genomic deletions and truncating mutations of the ANXA1 gene.[12,13] Because ANXA1 expression is reduced but not completely eliminated, deregulation may likely occur at the level gene transcription, suggesting that ANXA1 gene expression is governed by epigenetic changes, which may explain the frequent down-regulation in several cancers.

A major mechanism controlling cellular differentiation and the biological behaviour of cancer cells is the regulation of acetylation of lysine residues on the amino-terminal tails of histones. Histone acetylation modulates nucleosome and chromatin structure and regulates transcription factor accessibility and function.[14] The turnover of acetylation histones is regulated by the opposing activities of histone acetyltransferases (HAT) and histone deacetylases (HDAC), where HAT allow, while HDAC repress, transcription.[15] Importantly, deregulated histone HAT or HDAC activity has been found in certain human cancer (for a review see Ref. 16). In this manner, tumour cells are unable to undergo the normal cellular differentiation programme, which contributes to their neoplastic transformations. These findings suggest that the HAT/HDAC balance is a potential therapeutic target for human malignancy. Indeed, HDAC inhibitors (HDACi) have anti-proliferative and apoptotic effects on cancer cells. These effects are mediated in part by selective alternation in genes expression, such as induction of p21waf expression.[17] Several HDACi exhibit potent anti-tumour activity in human xenograft models, suggesting their usefulness as novel cancer therapeutic agents (for a review see Ref. 18). Moreover, because the spectrum of relevant HDAC inhibitor targetsin various types of human cancer has yet to be determined, itis not entirely clear which types of cancer are good candidatesfor further development of HDAC inhibitor therapy. Thus, further research in the identification of gene targets by HDACi is warranted. Recent data have indicated ANXA1 as a possible target of HDACi treatment. The depsipeptide FK228 has been shown to induce the expression and externalisation of ANXA1 in leukaemic cells, which in turn mediates the phagocytic clearance of apoptotic cells by macrophages. Induction of ANXA1 mRNA by FK228 was associated with histone acetylation in ANXA1 promoter.[19] Cyclopeptide FR235222 has been recently isolated from the fermentation broth of *Acremonium* sp.[20] The compound is a selective inhibitor of T cell proliferation and lymphokine production endowed with potent inhibitory activity of HDAC. As HDAC inhibitors are promising novel anti-cancer drugs, in this study we have investigated the mechanisms of the anti-proliferative and apoptotic effects of FR235222 in leukaemia cells and the putative role of ANXA1, in order to contribute to the clarification of the mechanism of action for correct therapeutic applications.

2. Materials and methods

2.1. Cell culture and reagents

Human promyelocytic leukaemia U937 cells, human chronic myelogenous leukaemia K562 cells and human T cell leukaemia Jurkat cells were provided by the American Type Culture Collection and maintained in RPMI 1640 medium supplemented with 2 mM L-glutamine, 10% heat-inactivated foetal bovine serum (FBS), 1% penicillin and 1% streptomycin (all from Cambrex Bioscience, Verviers, Belgium) at 37 °C in 5% CO_2 –95% air humidified atmosphere and plated in 100-mm tissue culture dishes (Falcon 3003, BD Biosciences). FR235222 was synthesised at the Department of Pharmaceutical Sciences, University of Salerno (Italy) as previously described.[21] The HDAC inhibitors suberoylanilide hydroxamic acid (SAHA) and trichostatin-A (TSA) were purchased from Sigma-Aldrich (Steinheim, Germany) and Alexis Biochemicals (Lausen, Switzerland). SAHA and TSA were dissolved in DMSO as stock solution, stored at –20 °C, and subsequently diluted with RPMI 1640 before use.

2.2. WST assay (cell growth assay)

To quantify cell proliferation, the sulfonated tetrazolium salt, 4-[3- (4-iodophenyl)-2-4-nitrophenyl]- 2H- 5- tetrazolio-1, 3-benzene disulfonate (WST-1) assay (Roche Molecular Biochemicals, Mannheim, Germany) was performed as described previously.[22] Cells were plated at a density of 3000 per well in 96-well plates in 100 l medium, and incubated for 72 h at 37 °C. 10 μl WST-1 reagent was then added into the cells and incubated for 2 h at 37 °C. Viable cell were estimated using a scanning multi-well spectrophotometer, with a test wavelength of 450 nm, against reference wavelength of 600 nm.

2.3. Analysis of cell cycle

The cells were plated at 2×10^5 in 60 mm dish, and exposed for 8 h, 24 h and 48 h to FR235222 (50 nM). Cells were harvested and fixed in cold 70% ethanol at –20 °C. Cell cycle profiles were evaluated by DNA staining with 2.5 mg/ml propidium iodide in phosphate-buffered saline (PBS) supplemented with 100 U/ml ribonucleases A, for 30 min at room temperature. Samples were analysed with a FACScan flow cytometer (Becton Dickinson, CA), using Mod FitLT program.

2.4. Analysis of apoptosis

Hypodiploid DNA was analysed using the method of propidium iodide (PI) staining and flow cytometry as described.[23] Briefly, cells were washed in phosphate-buffered saline (PBS) and resuspended in 500 μl of a solution containing 0.1% sodium citrate, 0.1% Triton X-100 and 50 μg/ml PI (Sigma-Aldrich).

2.5. Western blotting analysis

Expression of ANXA1 was examined by SDS-PAGE. Total intracellular protein was extracted from the cells by freeze/thawing in lysis buffer containing protease and phosphatase

inhibitors. Protein content was estimated according to Biorad protein assay (BIO-RAD, Milan, Italy). Expression of cell surface and intracellular ANXA1 was examined by SDS-PAGE. For cell surface protein the cells were first washed for 10 min on ice with PBS containing protease, phosphatase inhibitors and 5 mM EDTA that acts as a Ca^{2+} chelating agent and removes ANXA1 attached to cell surface. Samples (50 μg protein) were loaded onto 12% acrylamide gel and separated by SDS-PAGE. The separated proteins were then transferred electrophoretically to nitrocellulose paper (Immobilon-NC, Millipore, Bedford, USA). Proteins were visualised using the enhanced chemiluminescence detection system (Amersham Pharmacia Biotech) after incubation overnight at 4 °C with the following antibodies: rabbit polyclonal anti-histone H4 and acetylated histone H4 (Upstate Biotechnology, Lake Placid, NY), mouse monoclonal anti-p21, rabbit polyclonal anti-caspase-3 (Santa-Cruz Biotechnology, D.B.A. ITALIA s.r.l, Milan, Italy), rabbit polyclonal anti-cyclin E (Cell Signaling Technology, Denvers, MA), rabbit polyclonal anti-ANXA1 and rabbit polyclonal anti-ANXA1- serine[27] (kindly provided by Dr. Egle Solito, Imperial College, London, UK).

2.6. RNA extraction and Real-Time quantitative PCR analysis

Total RNA was extracted from cell cultures after different times of incubation with FR235222 50 nM (0, 4, 8 and 24 h), using TRIzol reagent (Invitrogen). 1 μg RNA from each sample was treated with DNase I (Invitrogen) and reverse transcribed using oligo (dT) primers and Superscript First Strand Synthesis System for RT-PCR (Invitrogen) according to the manufacturer instructions. Real-time PCR amplifications and analyses were performed on a Light-cycler system (Roche) using the LightCycler–FastStart DNA Master plus SYBR Green I kit (Roche Molecular Biochemicals, Mannheim, Germany). ANXA1 and the housekeeping gene GAPDH were amplified with specific primers. Sense primer for ANXA1 was 5′-ATCAGCGGTGAGCCCCTATC-3′, corresponding to nucleotides 173–192 and antisense primer was 5′-TTCATCCAGGGGC-TTTCCTG-3′, corresponding to nucleotides 356–337 of human ANXA1 cDNA sequence. Sense primer for GAPDH was 5′-AC-CCACTCCTCCACCTTTG-3′ corresponding to nucleotides 928–946 and antisense primer was 5′-CTCTTGTGCTCTTGCT-GGG-3′ corresponding to nucleotides 1087–1105 of human GAPDH cDNA sequence. Standard curves were generated from increasing amount of cDNA made from total control RNA. The C_T values were used to calculate a linear regression line by plotting the logarithm of template concentration (x-axis) against the C_T value (y-axis). These regression lines were used to calculate the expression level (ng of total RNA) for unknown samples. Expression levels of ANXA1 were normalised with GAPDH mRNA in each sample. All experiments were performed in triplicate.

2.7. Statistical analysis

All results are shown as mean ± SEM of three experiments performed in triplicate. The optical density of the bands of ANXA1, p21, cyclin E and caspase-3 protein expression detected by Western blotting was normalised with alpha-tubulin. Statistical comparison between groups was made using parametric Bonferroni test (GraphPad Prism, 4.01, 2004). Differences were considered significant if $p < 0.05$.

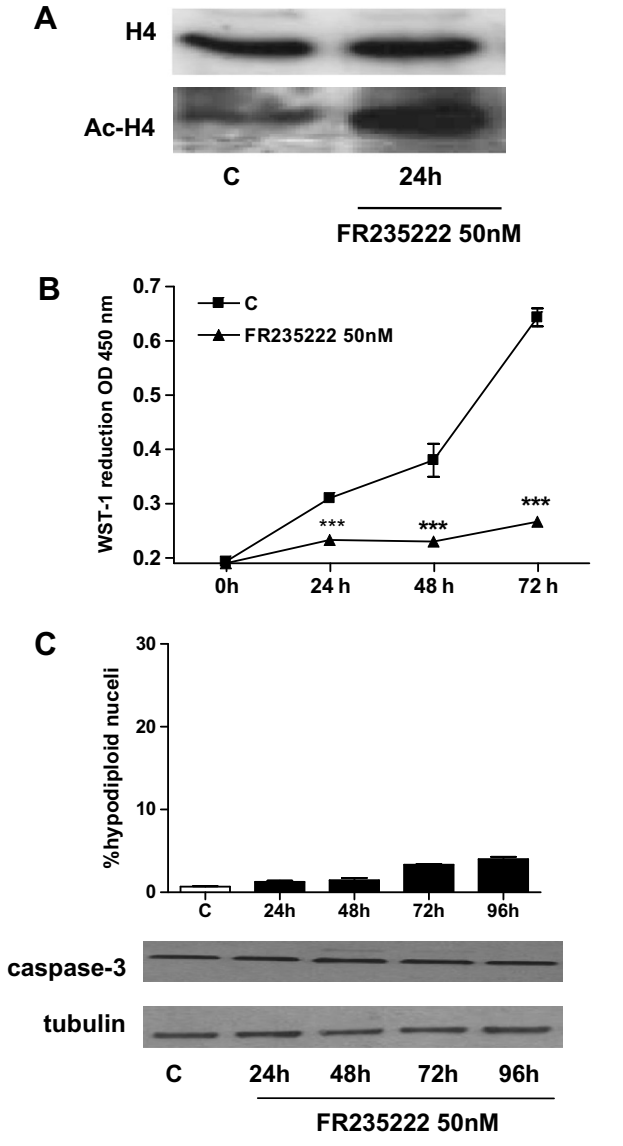

Fig. 1 – Effect of FR235222 on histone acetylation, cells growth and apoptosis. (A) U937 cells were treated with FR235222 (50 nM) for 24 h and histone H4 and acetyl-hystone H4 measured by Western blotting. (B) Proliferation of U937 cells was assessed in the presence of FR235222 (50 nM) in a 96-well plate format. Cells were incubated for 24, 48 and 72 h and pulsed for 2 h with WST-1. Absorbances were measured at 570 nm and expressed in relation to absorbances of control (untreated) cells. ***$P < 0.001$ versus control ($n = 3 \pm$ SEM). (C) U937 cells were treated with FR235222 (50 nM) for different times (0–96 h) and apoptosis was assessed by propidium iodide (PI) staining of hypo-diploid nuclei by flow cytometry ($n = 3 \pm$ SEM). Caspase-3 activation was assessed by Western blotting.

3. Results

3.1. FR235222 induces accumulation of acetylated histones and inhibits U937 cell proliferation

We first examined the effect of FR235222 on histone acetylation status in human promyelocytic leukaemia U937 cells. The cells were incubated with FR235222 (50 nM) for 24 h and protein extracts were used for Western blot analysis. Increased acetylation of histone H4 compared with controls was observed (Fig. 1A). The levels of histone H4 expression remained constant in U937 cells after treatment with FR235222. Acetylated histone H3 was not detected ($n = 3$ experiments, data not shown). We next investigated the effect of FR235222 on U937 cell proliferation. The cells were exposed to 50 nM FR235222 and their viability was followed for72 h using the WST-1 cell proliferation assay. Fig. 1B indicates that an exposure to FR235222 inhibited cellular proliferation at 24, 48 and 72 h ($p < 0.001$). Finally, we investigated the effect of FR235222 on U937 cell apoptosis. The cells were exposed to 50 nM FR235222 for different times. Apoptosis was measured by both cytofluorimetric analysis of PI staining of hypodiploid nuclei and caspase-3 activation by Western blotting. The results in Fig. 1C clearly indicate that 50 nM FR235222 had no effect on apoptosis in U937 cells up to 96 h.

3.2. FR235222 induces cell cycle arrest in the G1 phase via p21

To determine the mechanisms involved in growth inhibition induced by FR235222 we performed time kinetic studies of the cell cycle. Thus, U937 cells were exposed to 50 nM FR235222 for 8, 24 and 48 h and subjected to cell cycle analysis by FACS. Data in Fig. 2A indicate that 38% of the untreated cells were in the G0/G1 phase and 49.3% in the S phase. Treatment with FR235222 caused a time-dependent increase of the cell percent in the G0/G1 phase with a peak of 89.3% at 48 h as well as a reduction of the cell percent in the S phase (10.62% at 48 h). These data are consistent with a cell cycle arrest at the G0/G1 phase. Cell cycle progression is tightly regulated through a complex network of positive and negative regulatory molecules, such as cyclin-dependent kinases and cyclins. To elucidate the specific regulatory proteins responsible for the cell cycle arrest by FR235222 in U937 cells, protein extracts were prepared from cells treated at indicated time points.

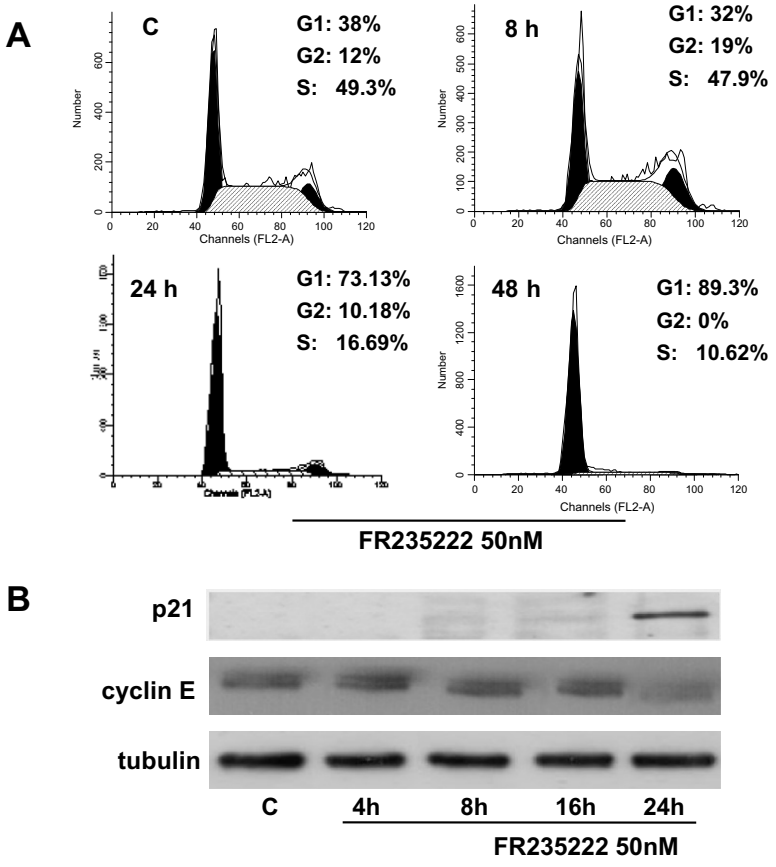

Fig. 2 – Effect of FR235222 on cell cycle and expression of cell cycle regulatory proteins in U937 cells. (A) Cell cycle analysis of U937 after exposure to FR235222 (50 nM) for 0 (Control), 8, 24 and 48 h. The U937 cells were incubated with PI and subjected to cell cycle analysis using a Becton Dickinson FACScan flow cytometer and ModFit software as described in Materials and Methods. (B) FR235222 (50 nM) was added for different times (0–24 h). At the end of the incubations, expression of p21 and cyclin E was measured by Western blotting.

FR235222 caused an increase of p21 at 24 h and a time-dependent decrease of cyclin E levels (Fig. 2B).

3.3. FR235222 stimulates the expression of ANXA1

ANXA1 inhibits cell proliferation in a number of unrelated cell types.[24] This negative regulation of cell proliferation involves the proximal modulation of ERK cascade, resulting in the sustained activation of this signal and in the arrest of cell growth via induction of the CDK2 inhibitor p21. Moreover, it has recently been shown that in ANXA1-overexpressing cells p21 protein expression is increased by haemin.[25] Therefore, we examined the possible role of ANXA1 in the FR235222-induced anti-proliferative effects in U937 cells. The cells were incubated with 50 nM FR235222 for different times. At the end of incubations, expression of ANXA1 was assessed by Western blotting. Fig. 3A shows that FR235222 significantly stimulated in a time-dependent fashion the expression of ANXA1 with peak effect at 24 h. Moreover, to verify whether the increase of ANXA1 expression was at the transcriptional level, quantitative PCR was used to analyse ANXA1 mRNA level in control U937 cells and in cells cultured for 4, 8 and 24 h in the presence of 50 nM FR235222. Fig. 3B shows that upon FR235222 treatment the levels of ANXA1 transcript were significantly increased by 20-fold at 24 h compared with untreated cells ($p < 0.001$). These results suggest that the augmented expression of ANXA1 may be responsible, at least in part, for the FR235222-induced growth arrest of U937 cells. Effect of 50 nM FR235222 on U937 cells was not associated with ANXA1 expression on plasma membrane (data not shown).

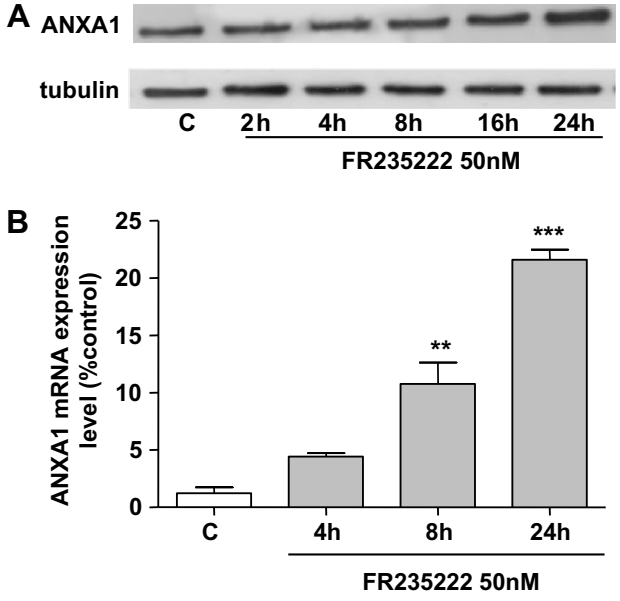

Fig. 3 – FR235222 stimulates ANXA1 expression. (A) U937 cells were incubated with FR235222 (50 nM) for different times (0–24 h). At the end of incubations, expression of ANXA1 was measured by Western blotting. (B) Real-time PCR analysis of ANXA1 gene expression was performed after 4, 8 and 24 h of incubation with 50 nM FR235222. ANXA1 mRNA levels are normalised with those of GAPDH and presented as % of the control, with the average of the controls set to 100%. $^{**}p < 0.01$ and $^{***}p < 0.001$ versus control ($n = 3 \pm$ SEM).

3.4. FR235222 inhibits cell proliferation and stimulates the expression of ANXA1 in Jurkat and K562 cell lines

We further evaluated FR235222 effects in other leukaemia cell lines, human chronic myelogenous leukaemia K562 cells and human T cell leukaemia Jurkat cells. In these cell lines FR235222 had similar effects to those observed in U937 cells (Fig. 4). An exposure to FR235222 (50 nM) inhibited cellular proliferation at 24, 48 and 72 h in both Jurkat (Fig. 4A) and K562 cells (Fig. 4E) and induced cell cycle arrest in the G1 phase in both Jurkat (Fig. 4B) and K562 cells (Fig. 4F). Moreover, FR235222 stimulated ANXA1 expression in both Jurkat (Fig. 4C) and K562 cells (Fig. 4G). Effects of 50 nM FR235222 on Jurkat and K562 cells were not associated with an ANXA1 expression on plasma membrane (data not shown). Finally, apoptosis was not induced by the compound in either cell line (Jurkat, Fig. 4D; K562, Fig. 4H).

3.5. SAHA and TSA induce ANXA1 expression in U937 cells

To investigate whether the up-regulation of ANXA1 expression is a unique property of FR235222 or is shared by other HDACi, U937 cells were treated with SAHA (1.5 μM) and TSA (250 nM) for 4, 8, 16 and 24 h and expression of ANXA1 evaluated by Western blotting. Data in Fig. 5A and D show that SAHA and TSA respectively stimulated ANXA1 expression in a time-dependent fashion suggesting that the effects on ANXA1 levels may be a common feature of this class of compounds. Furthermore, both SAHA (Fig. 5B) and TSA (Fig. 5E) induced cell cycle arrest at the G0/G1 phase in U937 cells but did not cause a significant apoptosis (Fig. 5C and F).

3.6. FR235222 induces apoptosis at high concentrations

As several HDACi have been reported to induce apoptosis in many tumour cell types (for a review see Ref. 26) we investigated whether FR235222 induced apoptosis in U937 cells at high concentrations. Cells were incubated as described in the Materials and Methods section with either vehicle (DMSO) or 0.5 μM FR235222 on the basis of concentration-response (data not shown). Results indicate that FR235222 stimulated apoptosis in U937 cells in a time-dependent fashion with peak effect at 48 h. Apoptosis was measured by both cytofluorimetric analysis of PI staining of hypodiploid nuclei (Fig. 6A) and by Western blotting of caspase-3 activation (Fig. 6B). The over-expression of ANXA1 in U937 cells has been shown to promote apoptosis associated with caspase-3 activation [4-5). Therefore, we determined the expression of ANXA1 in U937 cells stimulated with 0.5 μM FR235222 by Western blotting. As shown in Fig. 6C, FR235222 caused a time-dependent increase of full-length (37 kDa) ANXA1 levels accompanied by the detection of a N-terminal cleaved 33 kDa band in the cytosol. Increased full-length ANXA1 expression and the cleaved N-terminal ANXA1 were also detected on the plasma mem-

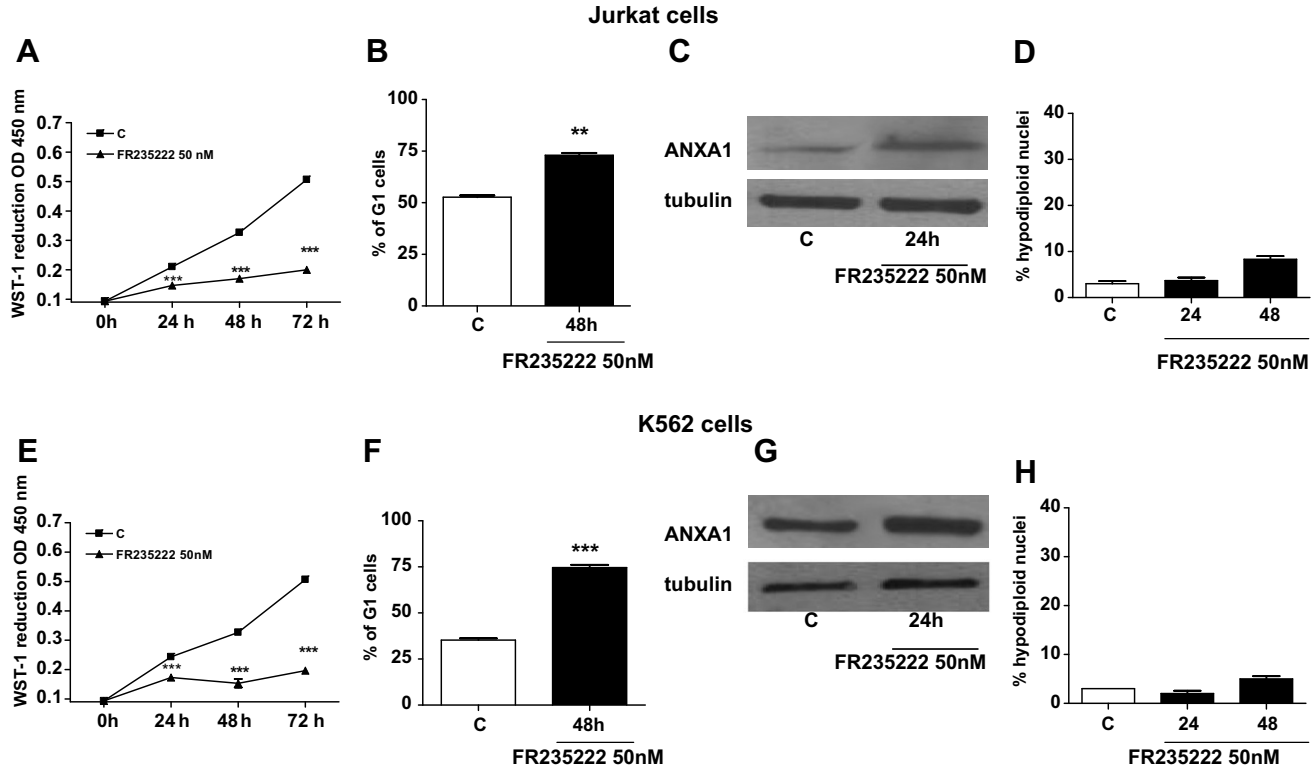

Fig. 4 – Effect of FR235222 on cell cycle, ANXA1 expression and apoptosis in Jurkat and K562 cells. FR235222 (50 nM) was added for different times as indicated. Proliferation of Jurkat (A) and K562 (E) cells were assessed in the presence of FR235222 (50 nM) in a 96-well plate format. Absorbances were measured at 570 nm and expressed in relation to absorbances of control (untreated) cells. $^{***}P < 0.001$ versus control ($n = 3 \pm$ SEM). The Jurkat (B) and K562 cells (F) were incubated with PI and subjected to cell cycle analysis using a Becton Dickinson FACScan flow cytometer and ModFit software as described in Materials and Methods. (C and G) Cytosol ANXA1 expression was measured by Western blotting. Apoptosis was assessed in Jurkat (D) and K562 (H) cells by propidium iodide (PI) staining of hypodiploid nuclei by flow cytometry.

brane (Fig. 6D). Recently it has been reported that translocation of full length ANXA1 to the cell membrane is dependent on serine[27] phosphorylation.[27] Therefore, we evaluated by Western blotting the presence on the plasma membrane the serine[27] phosphorylated ANXA1. As shown in Fig. 6D, FR235222 effect on U937 cells was also associated with a strong phosphorylation of 37 kDa ANXA1 at Ser-27 on plasma membrane. These results suggest that FR235222-induced apoptosis of U937 cells is associated with increased expression of ANXA1, protein processing and translocation to the membrane where it may act as an 'eat me' signal for macrophages.[28]

3.7. *Effects of FR23522 at high concentration in Jurkat and K562 cells*

To confirm the results obtained in U937 cells, we analysed the effects of 0.5 μM FR235222 in K562 and Jurkat cells. Results indicate that FR235222 stimulated apoptosis in both Jurkat (Fig. 7A) and K562 (Fig. 7C) cells in a time-dependent fashion with peak effect at 48 h. Apoptosis was measured by both cytofluorimetric analysis of PI staining of hypodiploid nuclei and caspase-3 activation by Western blotting. Moreover, 0.5 μM FR235222 caused an increase of 37 kDa ANXA1 levels in both Jurkat (Fig. 7B) and K562 cells (Fig. 7D), accompanied by the detection of a N-terminal cleaved 33 kDa band in the cytosol and on the plasma membrane.

4. Discussion

In the present paper, we evaluated the effects of the novel HDAC inhibitor FR235222 in a series of leukaemia cell lines. Initial investigations in U937 cells showed that treatment with 50 nM FR235222 caused accumulation of acetylated histone H4 and inhibition of cell proliferation. The anti-proliferative effect was related to the ability of FR235222 to cause growth inhibition at the G0/G1 phase transition of cell cycle. The G1 cycle arrest by FR235222 was accompanied by increase of p21 and down-regulation of cyclin E (see Fig. 2). The observed increase in the p21 level as well as the cell cycle arrest in the G1 phase suggests that FR235222 is a potent inhibitor of cell cycle progression. ANXA1 is a glucocorticoid-induced protein with a role in several patho-physiological processes. ANXA1 inhibits cell proliferation in a number of unrelated cell types acting via ERK activation [24]. Although ERK activation has been traditionally associated with increased cellular proliferation, many data suggest that sustained ERK activation, as observed in clones over-expressing ANXA1, can lead to expression of protein such as p21, culminating in cell cycle arrest.[29] Hence, ANXA1 may reduce proliferation by inducing

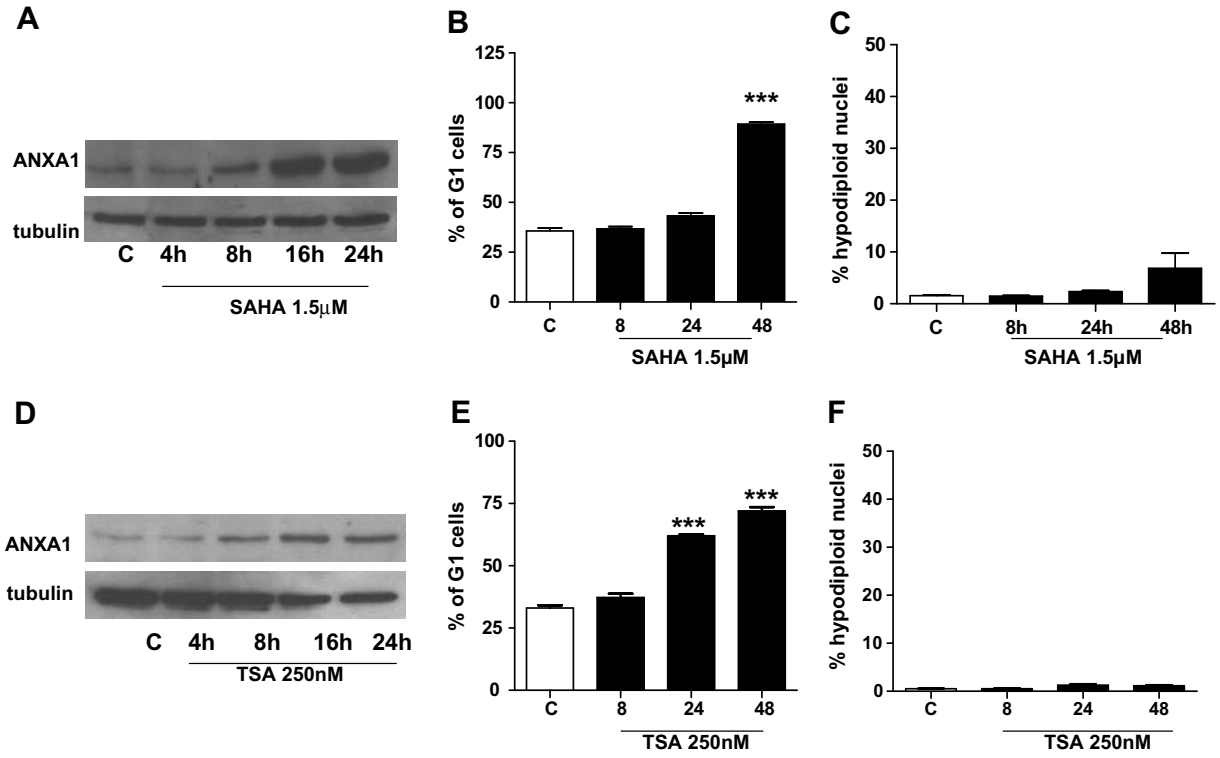

Fig. 5 – Effect of SAHA and TSA on ANXA1 expression, cell cycle and apoptosis. U937 cells were incubated with SAHA (1.5 μM) (A) and with TSA (250 nM) (D) for different times (0–24 h). Expression of ANXA1 at the end of incubations was measured by Western blotting. (B and E) U937 cells were incubated with PI and subjected to cell cycle analysis using a Becton Dickinson FACScan flow cytometer and ModFit software as described in Materials and Methods. $^{***}p < 0.001$ versus control ($n = 3 \pm$ SEM). (C and F) Apoptosis was assessed by propidium iodide (PI) staining of hypodiploid nuclei by flow cytometry.

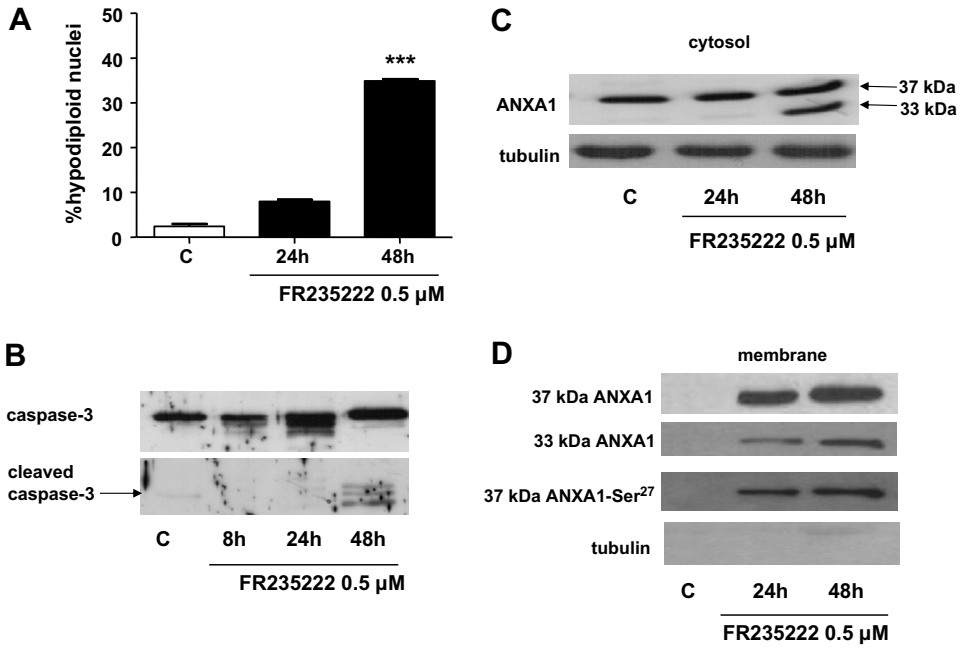

Fig. 6 – Effect of FR235222 at high concentrations on apoptosis and ANXA1 expression in U937 cells. U937 cells were cultured as indicated in Materials and Methods. FR235222 (0.5 μM) was added for different times as indicated. (A) Apoptosis was then assessed by propidium iodide (PI) staining of hypodiploid nuclei by flow cytometry. $^{***}p < 0.001$ ($n = 3 \pm$ SEM). (B) Caspase-3 activation was assessed by Western blotting. (C) Cytosol ANXA1 expression was measured by Western blotting. (D) Membrane ANXA1 expression and ANXA1 phosphorylation at Ser^{27} (37 kDa) were measured by Western blotting.

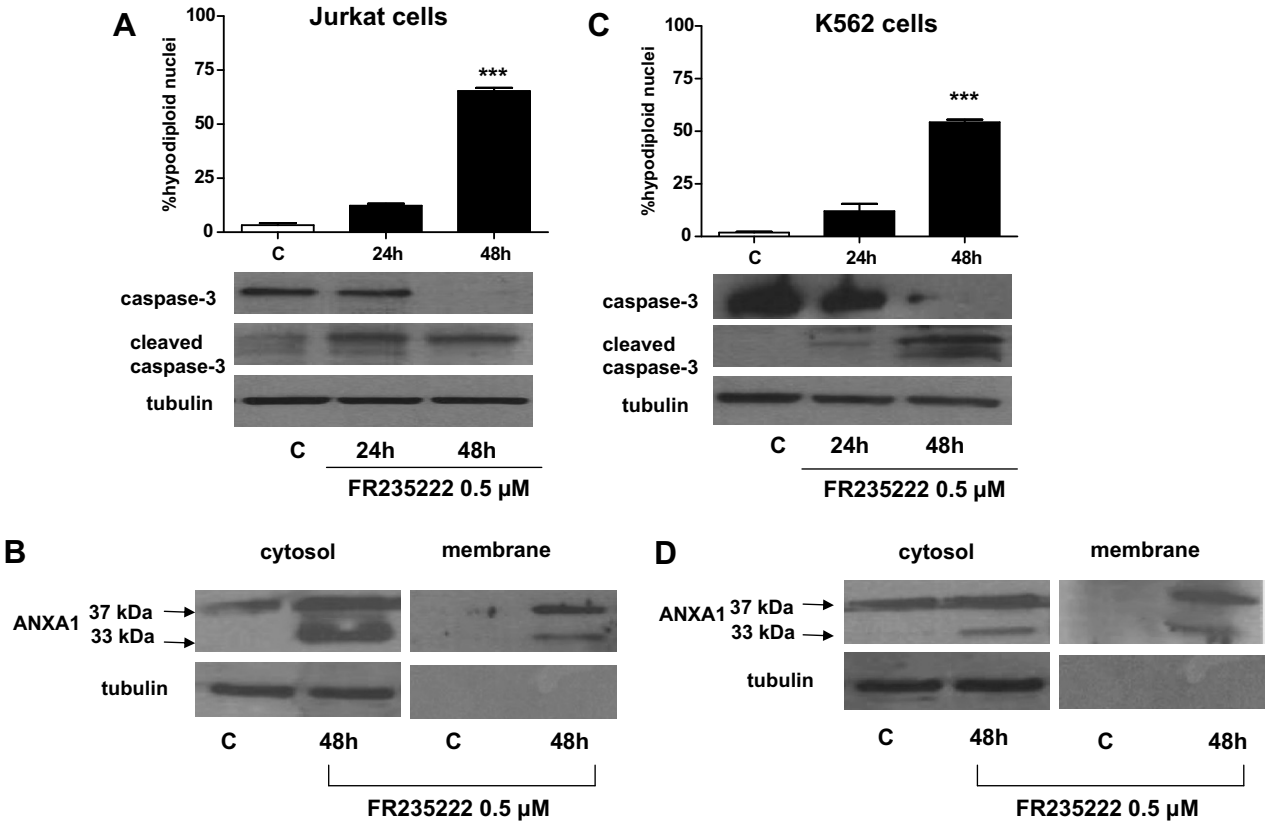

Fig. 7 – Effect of FR235222 at high concentrations on apoptosis and ANXA1 expression in Jurkat and K562 cells. Jurkat and K562 cells were cultured as indicated in Materials and Methods and FR235222 (0.5 μM) was added for different times as indicated. (A and C) Apoptosis was assessed by propidium iodide (PI) staining of hypodiploid nuclei by flow cytometry. $^{***}p < 0.001$ ($n = 3 \pm$ SEM). Caspase-3 activation was assessed by Western blotting. (B and D) Cytosol and membrane ANXA1 expression were measured by Western blotting.

the expression of p21 via constitutive activation of ERK. In agreement with these results, it has been recently reported that haemin-induced erythroid differentiation was blocked by ANXA1 knock down. The mechanisms of ANXA1-induced inhibition appeared to be related to increased ERK phosphorylation and p21 expression.[25] Therefore, we investigated the role of ANXA1 in the antiproliferative effects of FR235222 in U937 cells. FR235222 was able to increase the protein levels of ANXA1 in a time dependent fashion with a peak at 24 h. In addition, real-time PCR quantitative experiments showed a time-dependent increase of ANXA1 transcript levels by FR235222 indicating that the compound modulates ANXA1 gene expression in U937 cells at the transcriptional level. These results suggest that the inhibition of proliferation of U937 cells by FR235222 is mediated, at least in part, by ANXA1 via stimulation of p21 expression. The inhibition of cell proliferation and the up-regulation of ANXA1 expression by FR235222 shown in U937 cells were also observed in other leukaemia cell lines, human T cell leukaemia Jurkat cells and human chronic myelogenous leukaemia K562 cells (see Fig. 4), suggesting that in these cells also, ANXA1 may play a role in the anti-proliferative effects of FR235222. Interestingly, cycle arrest and up-regulation of ANXA1 expression were also observed in U937 cells treated with different HDAC inhibitors, like SAHA and TSA, indicating that these effects may be a common feature of this class of compounds.

Several HDACi have been reported to induce apoptosis in many tumour cell types. In our experiments 50 nM FR235222 had no effect on apoptosis of U937 cells up to 96 h incubation even in the presence of increased expression of ANXA1. Apoptosis was measured by both cytofluorimetric analysis of PI staining of hypodiploid nuclei and caspase-3 activation by Western blotting. The lack of effect on apoptosis by 50 nM FR235222 was also observed in Jurkat and K562 cells. Of note, the other HDAC inhibitors used in this study were also unable to induce significant apoptosis in U937 cells. In contrast, apoptosis was detected in U937 cells treated with high concentration (0.5 μM) FR235222 (see Fig. 6). Cell death was associated with an increased expression of the full-length (37 kDa) protein in both cytosol and membrane accompanied by the appearance of a 33 kDa N-terminal cleavage product. Furthermore, a serine[27] phosphorylated form of ANXA1 (37 kDa) was detected on the membrane in agreement with previous data showing that translocation of ANXA1 to the cell membrane is dependent on serine[27] phosphorylation.[27] Apoptosis accompanied by the appearance of the 33 kDa N-terminal cleavage product of ANXA1 in the cytosol and in the membrane was also induced by high doses

(0.5 μM) FR235222 in Jurkat and K562 cells. Very similar results have recently been reported by Tabe et al.[19] In AML1/ETO cells, HDAC inhibitor FK228 induced apoptosis accompanied by up-regulation of ANXA1 expression and translocation to the membrane of both the full-length protein and the 33 kDa N-terminal cleavage product.[25] Other authors have shown that over-expression of ANXA1 in U937 cells was associated to apoptosis with caspase-3 activation.[4,5] Taken together these observations suggest that the mere increase of ANXA1 expression is not sufficient to trigger apoptosis and that ANXA1 processing and subsequent appearance of the 33 kDa N-terminal cleavage product are instrumental in inducing apoptosis of leukaemia cells. Further experiments are needed to fully investigate the role of ANXA1 processing in cell death. Finally, the membrane expression of the protein in apoptotic cells is in agreement with previous data showing that ANXA1 is an 'eat-me' signal for macrophages[28] and that the protein and peptide derivatives stimulate the phagocytosis of apoptotic neutrophils by macrophages.[30] Thus, the translocation of ANXA1 to the membrane of apoptotic cells may represent a general mechanism of apoptotic cell clearance.

Conflict of interest statement

None declared.

Acknowledgements

This work was supported by grants from the University of Salerno (60% 2006, 2007), from the Italian Ministry of Research (COFIN 2006) to A.P. and L.P., and from BCC, Credito Cooperativo, Fisciano (Salerno). This paper is dedicated to the memory of Professor Luigi Gomez, prematurely deceased on April 5th 2006.

REFERENCES

1. Gerke V, Moss SE. Annexins: from structure to functions. *Physiol Rev* 2002;**82**:331–71.
2. Parente L, Solito E. Annexin 1. more than an anti-phospholipase protein. *Inflamm Res* 2004;**53**:125–32.
3. Lim LH, Pervaiz S. Annexin 1: the new face of an old molecule. *FASEB J* 2007;**21**:968–75.
4. Solito E, de Coupade C, Canaider S, Goulding NJ, Perretti M. Transfection of annexin 1 in monocytic cells produces a high degree of spontaneous and stimulated apoptosis associated with caspase-3 activation. *Br J Pharmacol* 2001;**133**:217–28.
5. Debret R, El Btaouri H, Duca L, et al. Annexin A1 processing is associated with caspase-dependent apoptosis in BZR cells. *FEBS Lett* 2003;**546**:195–202.
6. Hippo Y, Yashiro M, Ishii M, et al. Differential gene expression profiles of scirrhous gastric cancer cells with high metastatic potential to peritoneum or lymph nodes. *Cancer Res* 2001;**61**:889–95.
7. Kang JS, Calvo BF, Maygarden SJ, Caskey LS, Mohler JL, Ornstein DK. Dysregulation of annexin I protein expression in high-grade prostatic intraepithelial neoplasia and prostate cancer. *Clin Cancer Res* 2002;**8**:117–23.
8. Paweletz CP, Ornstein DK, Roth MJ, et al. Loss of annexin 1 correlates with early onset of tumorigenesis in esophageal and prostate carcinoma. *Cancer Res* 2000;**60**:6293–7.
9. Petrella A, Festa M, Ercolino SF, et al. Annexin-1 down-regulation in thyroid cancer correlates to the degree of tumour differentiation. *Cancer Biol Ther* 2006;**5**:643–7.
10. Garcia Pedrero JM, Fernandez MP, Morgan RO, et al. Annexin A1 down-regulation in head and neck cancer is associated with epithelial differentiation status. *Am J Pathol* 2004;**164**:73–9.
11. Xin W, Rhodes DR, Ingold C, Chinnaiyan AM, Rubin MA. Dysregulation of the annexin family protein family is associated with prostate cancer progression. *Am J Pathol* 2003;**162**:255–61.
12. Yen CC, Chen YJ, Chen JT, et al. Comparative genomic hybridization of esophageal squamous cell carcinoma: correlations between chromosomal aberrations and disease progression/prognosis. *Cancer* 2001;**92**:2769–77.
13. Fang Y, Guan X, Guo Y, et al. Analysis of genetic alterations in primary nasopharyngeal carcinoma by comparative genomic hybridization. *Genes Chromosomes Cancer* 2001;**30**:254–60.
14. Strahl BD, Allis CD. The language of covalent histone modifications. *Nature* 2000;**403**:41–5.
15. Gray SG, Teh BT. Histone acetylation/deacetylation and cancer: an "open" and "shut" case? *Curr Mol Med* 2001;**1**:401–29.
16. Marks PA, Richon VM, Miller T, Kelly WK. Histone deacetylase inhibitors. *Adv Cancer Res* 2004;**91**:137–68.
17. Johnstone RW, Licht JD. Histone deacetylase inhibitors in cancer therapy: is transcription the primary target? *Cancer Cell* 2003;**4**:13–8.
18. Glaser KB. HDAC inhibitors: Clinical update and mechanism-based potential. *BiochemPharmacol* 2007;**74**:659–71.
19. Tabe Y, Jin L, Contractor R, et al. Novel role of HDAC inhibitors in AML1/ETO AML cells: activation of apoptosis and phagocytosis through induction of annexin A1. *Cell Death Differ* 2007;**14**:1443–56.
20. Mori H, Urano Y, Abe F, et al. FR235222, a fungal metabolite, is a novel immunosuppressant that inhibits mammalian histone deacetylase (HDAC). I. Taxonomy, fermentation, isolation and biological activities. *J Antibiot (Tokyo)* 2003;**56**:72–9.
21. Rodriquez M, Terracciano S, Cini E, et al. Total synthesis, NMR solution structure, and binding model of the potent histone deacetylase inhibitor FR235222. *Angew Chem Int Ed Engl* 2006;**45**:423–7.
22. McCluskey C, Quinn JP, McGrath JW. An evaluation of three new-generation tetrazolium salts for the measurement of respiratory activity in activated sludge microorganisms. *Microb Ecol* 2005;**49**:379–87.
23. Nicoletti I, Migliorati G, Pagliacci MC, Grignani F, Riccardi C. A rapid and simple method for measuring thymocyte apoptosis by propidium iodide staining and flow cytometry. *J Immunol Methods* 1991;**139**:271–9.
24. Alldridge LC, Bryant CE. Annexin 1 regulates cell proliferation by disruption of cell morphology and inhibition of cyclin D1 expression through sustained activation of the ERK1/2 MAPK signal. *Exp Cell Res* 2003;**290**:93–107.
25. Huo XF, Zhang JW. Annexin1 regulates the erythroid differentiation through ERK signaling pathway. *Biochem Biophys Res Commun* 2005;**331**:1346–52.
26. Bolden JE, Peart MJ, Johnstone RW. Anticancer activities of histone deacetylase inhibitors. *Nat Rev Drug Discov* 2006;**5**:769–84.
27. Solito E, Christian HC, Festa M, et al. Post-translational modification plays an essential role in the translocation of annexin A1 from the cytoplasm to the cell surface. *FASEB J* 2006;**20**:1498–500.

28. Arur S, Uche UE, Rezaul K, et al. Annexin I is an endogenous ligand that mediates apoptotic cell engulfment. *Dev Cell* 2003;**4**:587–98.
29. Pumiglia KM, Decker SJ. Cell cycle arrest mediated by the MEK/mitogen-activated protein kinase pathway. *Proc Natl Acad Sci U S A* 1997;**94**:448–52.
30. Scannell M, Flanagan MB, deStefani A, et al. Annexin-1 and peptide derivatives are released by apoptotic cells and stimulate phagocytosis of apoptotic neutrophils by macrophages. *J Immunol* 2007;**178**: 4595–605.